Performance Measurements of Virtual Reality Systems: Quantifying the Timing and Positioning Accuracy

Paper ID #439

ABSTRACT

We propose the very first non-intrusive measurement methodology for quantifying the performance of commodity Virtual Reality (VR) systems. Our methodology considers the VR system under test as a black-box and works with any VR applications. Multiple performance metrics on timing and positioning accuracy are considered, and detailed testbed setup and measurement steps are presented. We also apply our methodology to several VR systems in the market, and carefully analyze the experiment results. We make several observations: (i) 3D scene complexity affects the timing accuracy the most, (ii) most VR systems implement the dead reckoning algorithm, which incurs a non-trivial correction latency after incorrect predictions, and (iii) there exists an inherent trade-off between two positioning accuracy metrics: precision and sensitivity.

1. INTRODUCTION

Virtual Reality (VR) renders computer-generated objects to create virtual environments for users [6], which enables many applications, such as military, healthcare, and video games, and thus becomes more and more popular. In fact, market research [3] indicates that the VR's annual market could grow to $80 billion in 10 years, compared to the current laptop computer market at $111 billion and game console market at $14 billion. The main driving force behind such a high growth rate is the *commodity* Head-Mounted Displays (HMDs) recently built for *desktop* and *mobile* VR systems, including Sony Morpheus, Microsoft HoloLens, Oculus Rift, and HTC Vive [1].

VR systems with HMDs were first built in research labs decades ago [14], using miniature Cathode Ray Tubes (CRTs) for displaying and mechanical/ultrasonic sensors for head tracking, in order to change the rendered images when the user moves. Over years, various hardware components have been enhanced for better VR experience at lower costs. Among these components, the compact and inexpensive Micro-Electro-Mechanical System (MEMS) sensors and high-resolution displays, which are also adopted by smartphones, allow VR developers, such as Oculus [7], to build commodity HMDs for VR systems. In these HMDs, the cumbersome mechanical/ultrasonic head-tracking sensors are replaced by MEMS inertial sensors with accelerometers and gyroscopes. However, these commodity VR systems suffer from *drifting* due to integration over potentially biased inertial sensor readings [15], which may be nontrivial as the sensors are likely to be inexpensive. This kind of drifting leads to *inaccurate* head-tracking results, which in turn cause cybersickness, like nausea, disorientation, headaches, sweating, and eye strain [4]. Hence, quantifying the performance of the commodity VR systems is crucial for faster and wider adoption.

Measuring the performance of the commodity VR systems is no easy task, because these HMDs are consumer-grade products with limited, if any, hardware and software accessibility. Moreover, these VR systems consist of multiple entities, including HMDs, rendering desktops or smartphones, VR applications, and dead reckoning algorithms. Since these entities all directly affect the system performance, we propose a system-wide black-box measurement methodology in this paper. Our methodology is general, because it does not: (i) instrument the VR systems (e.g., VR applications and HMDs) nor (ii) assume the existence of a specific (easy to recognize) virtual object. In other words, our methodology works with off-the-shelf VR systems, which to our best knowledge, is not possible in prior arts [5, 8, 10, 13]. Furthermore, our measurement methodology quantifies several variations of the *timing* and *positioning accuracy* metrics, which were not discussed in the literature. We apply the methodology to several commodity VR systems, and analyze the measurement results. Several observations are made from our experiment results: (i) 3D scene complexity affects the timing accuracy the most, showing the importance of rendering desktops or smartphones, (ii) most VR systems (3 out of 4) implement the dead reckoning algorithm, which shortens the time of reacting to head movements, but incurs a non-trivial correction latency after incorrect predictions, and (iii) there exists an inherent trade-off between two positioning accuracy metrics: some VR systems opt for higher precision, while others opt for higher sensitivity.

2. RELATED WORK

The implications of low-level VR system performance, such as latency, on high-level user experience have been studied using carefully-designed subjective tests. For example, Papadakis et al. [9] investigate the relation between spatial memory performance and latency. Young et al. [16] compare the performance of two VR systems by asking subjects to perform diverse tasks, such as sorting and searching, and provide opinion scores. Samaraweera et al. [12] study whether mobility impaired patients are less vulnerable to cybersickness due to the latency. These subjective experiments are complementary to our work that focuses on objective experiments on commodity VR systems.

There are few existing work proposing methodologies to measure the latency of VR systems. Papadakis et al. [10] present a system with photodiodes, an oscilloscope, and a servo-motor to measure the latency of a head-tracking (inertial) sensor. They manually read the measurement results from the oscilloscope, which may be error-prone. Steed [13] proposes to create a virtual pendulum, and configures it to follow a head-tracking sensor that moves in a sinusoidal pattern. The measured results of the pendulum and the head-tracking sensor are fit to sinusoidal functions, which are then used to calculate the latency. Di Luca [8] proposes to use two photodiodes to capture the position of the head-tracking sensor based on gradient images. The signals from photodiodes need to be processed, which may result in additional and unknown latency, and over-estimated latency. Friston and Steed [5] propose an automated frame counting approach to measure latency using an easily-recognized virtual object that follows the movement of a head-tracking sensor. They assume that this virtual object is never occluded by other objects. Compared to these studies [5, 8, 10, 13], our work: (i) considers a wider spectrum of performance metrics, and (ii) works with off-the-shelf VR applications in arbitrary scenes.

3. METHODOLOGY

Our proposed methodology controls the movements of an HMD, and measure the differences between the physical and virtual world states using off-the-shelf VR applications. We describe the design of testbed, performance metrics, measurement procedures, and post-processing steps in the rest of this section.

3.1 Testbed Setup

The measurement testbed comprises a number of components: (i) a rotating platform [2] to emulate head (HMD) movements, (ii) an external display that mirrors the view in the HMD, and (iii) a high-speed camera that captures both the HMD device and the HMD view. We aim to support both desktop and mobile VR systems. Desktop VR systems (such as Oculus Rift) have dedicated HMD devices, while mobile VR systems (such as Samsung Gear VR) directly use smartphones within cases that work as HMD devices. For brevity, we use HMD devices to refer to the devices that provide VR view in both desktop and mobile VR systems.

Figure 1 shows the testbed for Oculus Rift and Google Cardboard HMDs. As shown in this figure, the HMD device is mounted on the rotating platform. For desktop VR systems, we redirect the HMD view to an external display via an HDMI cable. For mobile VR systems, no external display is used, because the smartphone (Samsung S6) used in our testbed does not support any HDMI output. In either cases, the high-speed camera needs to shoot both the HMD device and the HMD view (either on the external monitor or the smartphone display). We use Apple iPhone 6 as the high-speed camera, which supports continuous 240 fps (frame-per-second) video recording. To emulate the movement of HMDs in action, a rotating platform is used to mimic various human head motions. The platform comes with a high-quality step motor, and is fast and accurate even when it is loaded with up to 10 KG objects. More specifically, the platform can rotate at angular speed from 0.001 rpm (revolutions per minute) to 200 rpm with a stepping resolution of 0.007°.

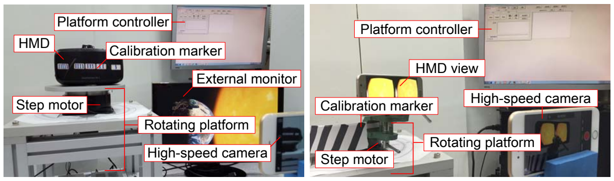

(a) with Oculus Rift

(b) with Google Cardboard

Figure 1: Testbed setup.

3.2 Performance Metrics

The basic requirement of a VR system is to track the physical motions and provide corresponding visual/multimodal feedbacks as realistic as possible. Hence, we quantify the performance of the VR systems in two aspects: timing and positioning accuracy.

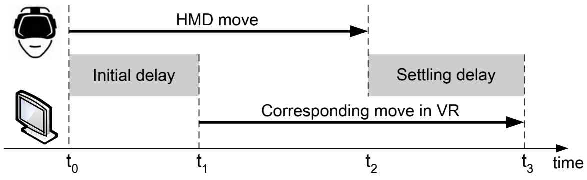

Figure 2: Illustrations of initial and settling delays in VR systems.

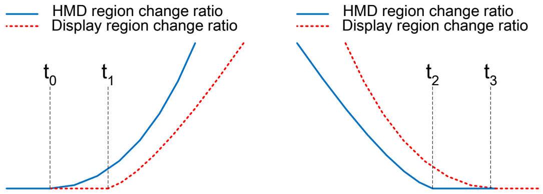

(a) based on the initial reference frame

(b) the settled reference frame

Figure 3: Detection of change points on the region change ratio time series.

Timing accuracy. Timing accuracy is critical as it is highly related to a variety of cybersickness, such as nausea, disorientation, and headaches. We define the following two metrics to quantify timing accuracy, which are also illustrated in Figure 2.

1. *Initial delay*: The time difference between the start of head motion (t_0) and that of the corresponding feedback in the virtual world (t_1).

2. *Settling delay*: The time difference between the stop of head motion (t_2) and that of the corresponding feedback in the virtual world (t_3).

Positioning accuracy: The spatial inconsistency between physical moves and visual feedback is another major cause of cybersickness. We accordingly define two metrics as follows.

3. *Precision*: The angular positioning consistency between physical moves and visual feedbacks in the virtual world in terms of degrees.

4. *Sensitivity*: The capability of HMD inertial sensors to perceive subtle motions and subsequently provide feedbacks to users.

3.3 Measurement Procedures

The measurement procedures for the four performance metrics are all similar, and are presented in the following. First, we select a VR application as the experiment scenario. Second, we configure the desired motion parameters that will be performed by the rotating platform, such as (angular) velocity and rotation angle. Last, we start both the rotating platform and high-speed camera to record the motion of the HMD and the HMD view. We recommend repeating each experiment at least 20 rounds for statistically meaningful results.

Since we rely on video recordings to monitor the HMD motions and the corresponding visual feedbacks on HMD view, it is important for the HMD view needs to be fully observable by the high-speed camera when the rotation starts and ends. This becomes an

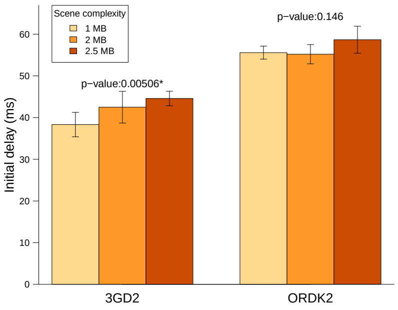

Figure 4: Initial delay under different scene complexities.

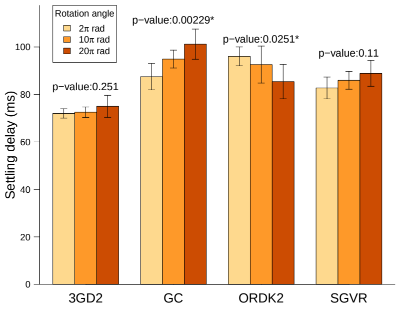

Figure 5: Settling delay under different rotation angles.

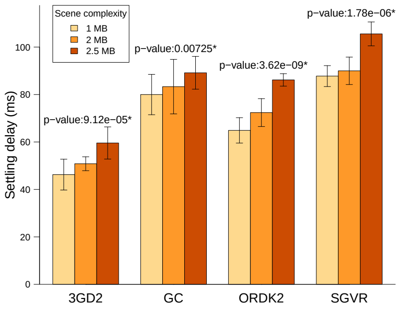

Figure 6: Settling delay under different scene complexities.

Table 1: The Considered Commodity VR Systems

Type	Desktop VR Systems		Mobile VR Systems	
Name	3Glasses D2	Oculus Rift DK2	Google Cardboard	Samsung Gear VR
Dim. (mm)	192.5×88×88	181×120.5×91	154.5×88.5×81	201.9×166.4×92.6
Weight (g)	246	440	213	446
FoV (°)	110	100	96	96
Display	2560×1440, 60 Hz	2560×1440, 75 Hz	2560×1440, 60 Hz	
CPU	Intel i7-4790 CPU 3.60 GHz		4-core Cortex-A57 2.1 GHz and 4-core Cortex-A53 1.5 GHz	
GPU	GeForce GTX 645		Mali-T760 MP8	
RAM	32 GB		3 GB	

issue if the HMD does not support the mirroring of its view to an external display. For example, as Samsung S6 does not support external displays, the rotation angles have to be multiples of 2π, so that the HMD stops at approximately the same position as where it starts. Similarly, we cannot measure the initial delay on these HMDs. A possible workaround is to fixate the high-speed camera on the rotating platform, but the vibrations of the platform lead to blur videos, in our experience. Hence, currently the initial delay is not measured for mobile VR systems that do not support external monitors.

3.4 Post-processing Steps

Several post-processing steps need to be performed to extract the performance results. The input to the post-processing steps is the recorded video from the high-speed camera. Since each experiment consists of multiple repeated rounds (say N), we leverage the sound made by the rotating platform (i.e., the step motor) to cut the video recording in N clips. Furthermore, the video clips are converted to gray scale before the content analysis, which is detailed below.

First, we need to derive two reference frames from each video clip. The *initial reference frame* is derived as the average of the first K frames[1], where the *settled reference frame* is derived as the average of the last K frames in each video clip. For each reference frame, we define two regions: (i) *the HMD region*, which comprises the calibration marks on the HMD or on the upper tray of the rotating platform (see Figure 1) across video frames. The purpose of the calibration marks is to add some salient points on the rotating platform and HMD so that the angular changes of HMDs can be easily identified; (ii) *the display region*, which comprises the HMD view on the video frame.

Next, for a reference-frame-and-region pair (F, R), we compute the *region change ratio* in percentage of the changed pixels in the region R compared with the reference frame F, where a pixel is considered changed if the pixel's gray level is significantly different from that of the same pixel on the reference frame F[2].

Timing accuracy. We first obtain four time series based on the combinations of two regions and two reference frames. We then apply the change point detection algorithm [11] to automatically identify t_0 and t_2 from the region change ratios based on the initial reference frame, and t_1 and t_3 from those based on the settled reference frame. The derivations are summarized in Figure 3.

Positioning accuracy. The precision is computed as the region change ratio of the display region by comparing the initial and settled reference frames. The sensitivity is computed as the ratio of *sensible rounds* in all the rounds; a round is considered as sensible, if we can find any difference in the display region between the initial and settled reference frames.

4. EXPERIMENTS

4.1 Considered VR Systems

We compare the performance of four commodity VR systems, as illustrated in Table 1, which are available at the time of writing. 3Glasses D2 (3GD2) and Oculus Rift DK2 (ORDK2) are desktop VR systems connected to an Intel i7 PC via HDMI and USB cables for rendering 3D scenes. Google Cardboard (GC) and Samsung Gear VR (SGVR) are mobile VR systems that work with smartphones. GC is a chassis that holds a smartphone and lenses for low-cost VR experience. In contrast, SGVR dictates a Samsung smartphone connected via micro USB. We use Samsung S6 in GC and SGVR for rendering 3D scenes, because it is supported by both VR systems.

4.2 Experiment Results

We repeat each experiment 20 times with individual VR systems. The two major parameters are rotation angle (in rad) and velocity (in rad/s) If not otherwise specified, we set the angle as $\pi/2$ and the velocity as π.

Initial delay. We compare the initial delay of desktop VR systems under different rotation angles from 2π to 20π rad. We find the initial delay remains very similar: about 44 ms and 48 ms for 3GD2 and ORDK2[3]. We also compare the initial delay under different velocities from $\pi/8$ to π rad/s, and observe no clear difference. Figure 4 shows the initial delay under different scene com-

[1] We empirically choose $K = 100$ and find that the results are not sensitive to the K values.

[2] The threshold for the gray level difference is empirically set to 30 (in the range of 0–255).

[3] Figures that carry less information are not shown throughout this paper, due to the space limitations.

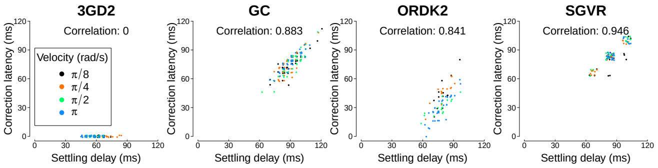

Figure 7: Correlation between correction latency and settling delay.

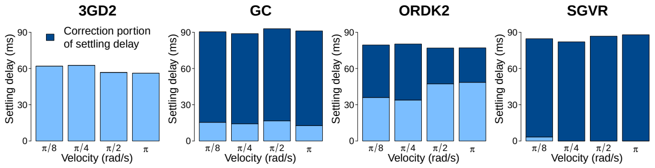

Figure 8: Portion of correction latency in settling delay.

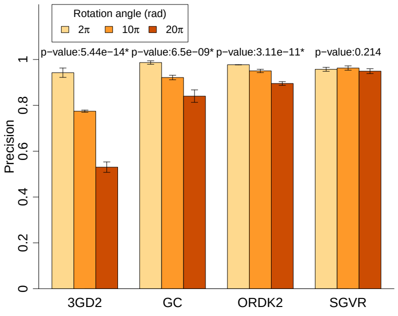

Figure 9: Precision under different rotation angles.

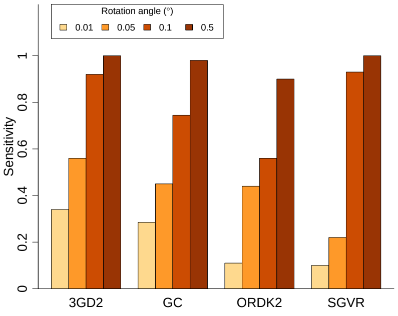

Figure 10: Sensitivity under different degrees per move.

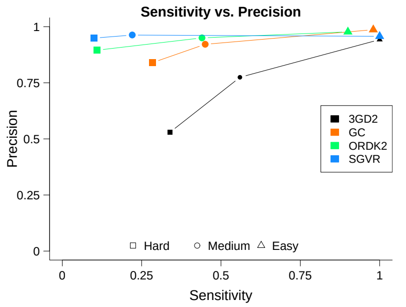

Figure 11: Trade-off between precision and sensitivity under 3 sample settings.

plexities, which are quantified by compressing each screenshot image into jpeg at quality level of 85%. We observe that: (i) higher complexity results in longer initial delay, and (ii) ORDK2 tends to have a slightly longer initial delay.

Settling delay. We next compare the settling delay of all four VR systems. Figure 5 reports the settling delay under different rotation angles. This figure shows that most VR systems (except ORDK2) suffer from longer settling delay under larger rotation angles. The unique behavior of ORDK2 may be attributed to the unique *kinematic constraints* [7] implemented in it. The implication of velocity on the settling delay is not clear in our experiments. The VR systems sorted in the descending order of settling delay are GC (90 ms), SGVR (80 ms), ORDK2 (75 ms), and 3GD2 (60 ms). Figure 6 gives the settling delay under different scene complexities. We observe that, similar to initial delay, higher complexity leads to longer settling delay. Moreover, desktop VR systems generally result in shorter settling delay than mobile VR systems, which can be attributed to: (i) less expensive inertial sensors and (ii) lower computational power of smartphones.

Correction latency. Next, we quantify the correction latency, which is mostly due to the dead reckoning algorithm. Figure 7 gives the scatter plots between correction latency and settling delay of individual VR systems. We make a critical observation: the correlation between the correction latency and settling delay are highly correlated in most VR systems, except 3GD2. In fact, 3GD2 always has *zero* correction latency, showing that *no* dead reckoning algorithm is implemented in 3GD2. Figure 8 gives the fraction of the correction latency in the settling delay. This figure reveals that in most VR systems (except 3GD2), especially mobile VR systems, correction latency represents a nontrivial portion of settling delay. Moreover, we find the correction latency is quite diverse on different VR systems: from about 40 ms in ORDK2 to about 80 ms and 90 ms in SGVR and GC. The correction latency is one of the side effect of the dead reckoning algorithm. We also conduct rigorous experiments to quantify the benefit of the dead reckoning algorithm. Due to the space limitation, we only give a high-level sample observation: thanks to the dead reckoning algorithm, ORDK2 reacts to head movements sooner and displays the same 3D scenes about 10 ms earlier than 3GD2 on average.

Precision and sensitivity. We vary the rotation angles from 2π to 20π rad, and plot the precision of the four VR systems in Figure 9. This figure depicts that the VR systems sorted by the precision in the descending order are SGVR, ORDK2, GC, and 3GD2. Such diversity of precision may be attributed to the design choices, e.g., some developers may prefer very high precision and filter out small noises (or movements). To verify this, we next vary the degree per move from 0.01 to 0.5, and plot the sensitivity of the four VR systems in Figure 10. This figure confirms our conjecture: VR systems that achieve higher precision, also suffer from lower sensitivity in general. To better visualize such trade-off, we select three sample settings on precision and sensitivity as follows. *Hard* is 20π rad and 0.01 degree per move; *medium* is 5π and 0.05; and *easy* is π and 0.5. The results are given in Figure 11. We make two observations from this figure. First, all VR systems perform well under the easy setting. Second, curves closer to the lower-right corner represent more sensitive, but less precise VR systems. That is, 3GD2 is the most sensitive VR system, while SGVR is the most precise one.

5. CONCLUSION

We presented a measurement methodology to quantify the timing and positioning accuracy of commodity VR systems. Our methodology considers the VR system under test as a black-box and works with any VR applications without code instruments and system modifications. We applied the methodology to four commodity VR systems to demonstrate its effectiveness. Several interesting observations were made from our experiments. For example, some VR systems opt for higher precision at the expense of lower sensitivity, while others prefer higher sensitivity and lower precision. Our proposed methodology may be leveraged by VR researchers and developers to better quantify the system-wide performance in both objective and subjective experiments.

6. REFERENCES

[1] HTC Vive vs Oculus Rift vs PlayStation VR. http://www.itpro.co.uk/desktop-hardware/25186/htc-vive-vs-oculus-rift-vs-playstation-vr-big-three-set-to-drive-just-13-per.

[2] Rotating platform specification. http://www.extion.com.tw/c/pdf/1/usc.pdf.

[3] Virtual reality could become an $80b industry: Goldman. http://www.cnbc.com/2016/01/14/virtual-reality-could-become-an-80b-industry-goldman.html.

[4] S. Davis, K. Nesbitt, and E. Nalivaiko. A systematic review of cybersickness. In *Proc. of Australasian Conference on Interactive Entertainment (IE'14)*, pages 1–9, Newcastle, Australia, December 2014.

[5] S. Friston and A. Steed. Measuring latency in virtual environments. *IEEE Transactions on Visualization and Computer Graphics*, 20(4):616–625, April 2014.

[6] D. Krevelen and R. Poelman. A survey of augmented reality technologies, applications and limitations. *The International Journal of Virtual Reality*, 9(2):1–20, January 2010.

[7] S. LaValle, A. Yershova, M. Katsev, and M. Antonov. Head tracking for the Oculus Rift. In *Proc. of IEEE International Conference on Robotics and Automation (ICRA'14)*, pages 187–194, Hong Kong, China, May 2014.

[8] M. D. Luca. New method to measure end-to-end delay of virtual reality. *Presence*, 19(6):569–584, December 2010.

[9] G. Papadakis, K. Mania, M. Coxon, and E. Koutroulis. The effect of tracking delay on awareness states in immersive virtual environments: An initial exploration. In *Proc. of ACM International Conference on Virtual Reality Continuum and Its Applications in Industry (VRCAI'11)*, pages 475–482, Hong Kong, China, December 2011.

[10] G. Papadakis, K. Mania, and E. Koutroulis. A system to measure, control and minimize end-to-end head tracking latency in immersive simulations. In *Proc. of ACM International Conference on Virtual Reality Continuum and Its Applications in Industry (VRCAI'11)*, pages 581–584, Hong Kong, China, December 2011.

[11] K. Rebecca and E. Idris. changepoint: An r package for changepoint analysis. *Journal of Statistical Software*, 58(3):1–19, 2014.

[12] G. Samaraweera, R. Guo, and J. Quarles. Head tracking latency in virtual environments revisited: Do users with multiple sclerosis notice latency less? *IEEE Transactions on Visualization and Computer Graphics*, 22(5):1630–1636, May 2016.

[13] A. Steed. A simple method for estimating the latency of interactive, real-time graphics simulations. In *Proc. of ACM Symposium on Virtual Reality Software and Technology (VRST'08)*, pages 123–129, Bordeaux, France, October 2008.

[14] I. Sutherland. A head-mounted three dimensional display. In *Proc. of Fall Joint Computer Conference (AFIPS'68)*, pages 757–764, San Francisco, CA, December 1968.

[15] G. Welch and E. Foxlin. Motion tracking: No silver bullet, but a respectable arsenal. *IEEE Computer Graphics and Applications*, 22(6):24–38, November/December 2002.

[16] M. Young, G. Gaylor, S. Andrus, and B. Bodenheimer. A comparison of two cost-differentiated virtual reality systems for perception and action tasks. In *Proc. of ACM Symposium on Applied Perception (SAP'14)*, pages 83–90, Vancouver, Canada, August 2014.